

Addressing Key Challenges of Adversarial Attacks and Defenses in the Tabular Domain: A Methodological Framework for Coherence and Consistency

Yael Itzhakev^{a,*}, Amit Giloni^a, Yuval Elovici^a and Asaf Shabtai^a

^aDepartment of Software and Information Systems Engineering, Ben-Gurion University of the Negev, Beer-Sheva, 8410501, Israel

ARTICLE INFO

Keywords:

Adversarial attacks
Tabular data
Machine learning
XAI
Security
Anomaly detection

ABSTRACT

Machine learning models trained on tabular data are vulnerable to adversarial attacks, even in realistic scenarios where attackers have access only to the model's outputs. Researchers evaluate such attacks, by considering metrics like success rate, perturbation magnitude, and query count. However, unlike other data domains, the tabular domain contains complex interdependencies among features, presenting a unique aspect that should be evaluated: the need for the attack to generate coherent samples and ensure feature consistency for indistinguishability. Currently, there is no established methodology for evaluating adversarial samples based on these criteria. In this paper, we address this gap by proposing new evaluation criteria tailored for tabular attacks' quality; we defined anomaly-based framework to assess the distinguishability of adversarial samples and utilize the SHAP explainability technique to identify inconsistencies in the model's decision-making process caused by adversarial samples. These criteria could form the basis for potential detection methods and be integrated into established evaluation metrics for assessing attack's quality. Additionally, we introduce a novel technique for perturbing dependent features while maintaining coherence and feature consistency within the sample. We compare different attacks' strategies, examining black-box query-based attacks and transferability-based gradient attacks across four target models. Our experiments, conducted on benchmark tabular datasets, reveal significant differences between the examined attacks' strategies in terms of the attacker's risk and effort and the attacks' quality. The findings provide valuable insights on the strengths, limitations, and trade-offs of various adversarial attacks in the tabular domain, laying a foundation for future research on attacks and defense development.

1. Introduction

Machine learning (ML) models trained on tabular data are widely deployed in diverse industry sectors including finance (e.g., for computing credit risk) [11, 36], healthcare (e.g., for analyzing administrative claims and patient registry data) [12], and energy (e.g., for predicting energy and electricity consumption) [28, 42]. However, recent research has highlighted their vulnerability to adversarial attacks, in which malicious data samples are used to mislead the model into producing incorrect outputs [2, 7, 35, 19]. For instance, an applicant may slightly increase his reported income (influencing the 'income level' feature), crossing a decision threshold and thereby changing the model's decision from "reject" to "approve." Such adversarial attacks can even be conducted in realistic black-box settings, where the attacker has no knowledge of the model's internals and can only query the model to receive outputs.

While extensive research has been performed in the image [49, 50, 24, 41], audio [29], text [49, 34, 18], and graph data [49, 45] domains, the tabular data domain remains relatively underexplored. This paper addresses several key challenges in the realm of adversarial attacks, focusing on tabular data.

Crafting Coherent and Consistent Adversarial Samples: Crafting adversarial samples in the tabular domain

presents unique challenges compared to other data types, such as images, where features (pixels) are typically independent and within a fixed range. Tabular data involves diverse feature types and Tabular models often rely on interdependent features, where the values of some features (dependent features) are influenced by others (influencing features). To maintain coherence and avoid detection, perturbations of dependent features must align with the values of other features. For example, 'BMI' is derived from 'height' and 'weight'. When modifying these influencing features (i.e., 'height,' 'weight,' or both) during an attack, it is important to ensure that the 'BMI' value remains consistent with the changes made to these features.

While the dependencies of 'BMI' are well-defined, there are cases where dependencies are indirect or influenced by unknown features. For example, 'diabetes risk level' depends on 'age,' 'BMI,' 'family history of diabetes,' and 'blood sugar levels.' In a practical scenario, the influential features may be hidden from the attacker, who might also lack precise knowledge of how the 'diabetes risk level' is determined based on them. Therefore, maintaining coherence and consistency within the adversarial sample during the perturbation process becomes particularly challenging.

Evaluation Criteria for Distinguishable Adversarial Samples: Existing evaluation methods for adversarial samples have primarily focused on measuring the perturbation magnitude using L_p norms, which are intended to indicate the level of detectability (i.e., the risk that the attack will be exposed). However, in the context of tabular data, simply

*Corresponding author

✉ freidiya@post.bgu.ac.il (Y. Itzhakev)

ORCID(S): 0009-0009-9854-8480 (Y. Itzhakev)

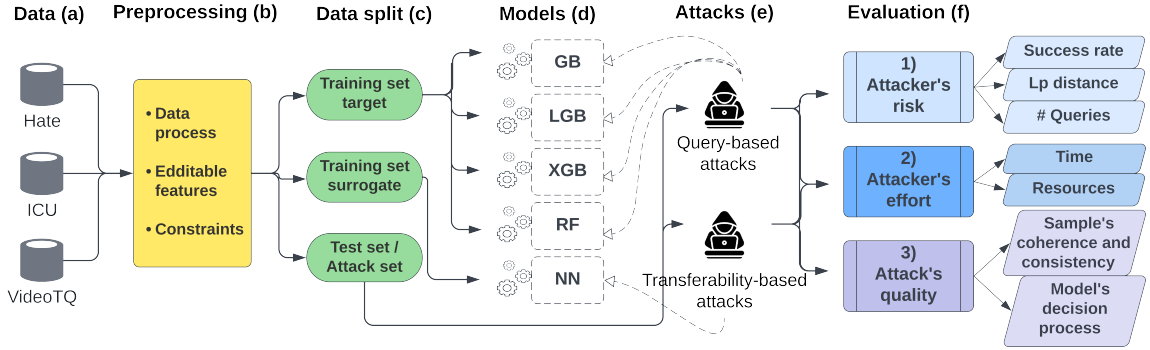


Figure 1: An overview of the paper’s methodological framework.

limiting perturbation magnitudes is insufficient. Effective adversarial attacks must ensure that samples remain coherent, consistent, and in-distribution to evade detection. While previous work has acknowledged these challenges (see Section 2.1), there is a lack of concrete evaluation methods for quantifying the distinguishability of adversarial samples generated by different attacks in the tabular domain.

Empirical Analysis of Different Attacks’ Strategies:

While adversarial attacks have been extensively studied in other domains, the analysis of black-box attacks’ strategies in the tabular domain has been limited. Common black-box attacks’ strategies are query- and transferability-based. In query-based attacks [7], the attacker repeatedly queries the target model, learns its decision boundary from the responses, and optimizes an adversarial sample to mislead it, while in transferability-based attacks [35, 19], the attacker optimizes the adversarial sample to mislead a *surrogate* model, and then uses this sample to mislead the target model with a single query.

Adversarial attacks are used by both defenders and attackers both of whom may choose different attacks’ strategies based on their goals, resources, and constraints. *Defenders* who are interested in assessing their models’ vulnerability often use adversarial attacks for automated penetration testing or adversarial training, which involves creating adversarial samples to improve the model’s robustness [10, 21]. Since defenders have full access to their models and can make unlimited queries, query-based attacks are a practical option. In contrast, *attackers* aiming to minimize queries and avoid detection might prefer transferability-based attacks that use gradient methods on neural networks, as these capture underlying feature interactions necessary for subtle perturbations. Understanding how and whether query-based attacks reflect other attack types, such as transferability-based gradient attacks, is crucial when using them to improve model defenses.

In this paper, we aim to advance adversarial research in the tabular domain by addressing existing gaps in the literature. We compare attacks’ strategies to provide insights for both attackers and defenders and propose a new technique for consistent perturbation of dependent features and concrete evaluation criteria for assessing attacks’ quality. We

perform a detailed examination of both black-box query- and transferability-based gradient attacks, tailored to respect tabular distribution constraints.

To address the challenge of crafting coherent and consistent adversarial samples, we introduce a novel technique for perturbing dependent features. This technique uses *regression models* to correct perturbed features during the attack process, ensuring that they remain consistent with the overall sample (see Section 3).

Additionally, we propose two concrete criteria for the assessment of attacks’ distinguishability and quality (see Section 3), which can also serve as potential detection mechanisms:

1. *Anomaly Assessment*: Measures the anomaly detection rate of adversarial samples compared to benign samples using isolation forest algorithm and autoencoder.
2. *Explainability-Based Analysis*: Identifies inconsistencies in the model’s decision-making process caused by adversarial samples, using an anomalous criteria based on SHapley Additive exPlanations (SHAP) [32], which is a commonly used explainability (XAI) technique [3].

Our comparison of attacks’ strategies integrates both traditional metrics of the attacker’s risk (success rate, query count, and L_p norms) and effort and the new evaluation criteria introduced in this paper, providing a thorough assessment of adversarial sample quality and attack effectiveness.

Four different target models were used to explore and evaluate the attacks’ strategies (process illustrated in Fig. 1) on three datasets: the Hateful Users on Twitter [43] and Intensive Care Unit [20] public datasets, which are both benchmark datasets in the tabular domain, and the Video Transmission Quality (VideoTQ) dataset, which is a private dataset. Seven attacks were examined in our evaluation: two well-known query-based attacks (the boundary and Hop-SkipJump attacks [5, 8] that can be adapted for tabular data [7]) and five transferability-based gradient attacks that varied in terms of their feature selection techniques (a basic attack [35] in which features were randomly selected and

four attacks in which features were selected based on their importance [19]).

This work sheds light on the key trade-offs between these attacks for the tabular domain, which can guide the selection of attacks’ strategies and motivate the development of new defense approaches tailored to the unique properties of this domain.

The contributions of our work can be summarized as follows:

- We introduce a novel technique for perturbing dependent features while maintaining coherence and ensuring feature consistency with the rest of the features.
- We propose two evaluation criteria to assess the distinguishability and quality of adversarial samples in the tabular domain, which can also assist the research community in developing more robust and effective attacks and defenses.
- To the best of our knowledge, this is the first study that thoroughly evaluates the characteristics of and differences between different attacks’ strategies in tabular data domains, which potentially impact defense strategy decisions.
- The resources of this study (preprocessed data, code, models, and adversarial samples) will be publicly released to promote future research.

The remainder of this paper is organized as follows: In Section 2, we discuss related work. Section 3 introduces our methodological framework, followed by Section 4 and Section 5, which present the experimental setup and provide a thorough analysis of the examined query- and transferability-based attacks’ behavior. Finally, Section 6 and Section 7 conclude with insights for attackers and defenders within tabular data domains.

2. Background and Related Work

2.1. State-of-the-Art Adversarial Attacks in Tabular Data Domains

Szegedy *et al.* [46] introduced the concept of an adversarial attack in which an attacker provides a malicious data sample aimed at misleading the ML model and causing it to produce incorrect output. Their adversarial sample was crafted by performing subtle changes to an image, which were imperceptible to the human eye but misled the target model. However, research conducted in tabular subdomains, such as fraud detection and recommendation systems [2, 7, 13], has highlighted additional critical challenges within the tabular domain. These challenges include the constraints of editable and non-editable features (e.g., ID, date of birth), data imbalance, and the presence of noncontinuous features (e.g., categorical features). The authors of these studies also mentioned the complexity of perturbing discrete values while maintaining the semantic integrity of the sample, as well as capturing nuances when designing attacks. This discussion was further elaborated on in [35].

Most recent adversarial attacks were demonstrated under black-box conditions (i.e., the attacker has no prior knowledge of the target model and only has the ability to query it [33]). The main types of black-box attacks are query-based attacks and transferability-based attacks.

In query-based attacks, the attacker assumes that the target model can be queried multiple times, and when queried, the attacker receives the model’s confidence or classification. The attacker iteratively adjusts the sample’s values, based on the model’s output, until the optimization objective is fulfilled - the target model is misled and produces the desired output. Decision-based attacks are examples of black-box query-based attacks [6]. These attacks typically involve making a large initial modification to the original sample, such that the target model produces an incorrect prediction. Then the attacker optimizes the modified sample’s values so they are as close as possible to the original sample while still misleading the target model. For evaluation, we implemented two decision-based attacks: The boundary attack and the HopSkipJump attack, which differ in terms of the extent of the initial changes made to the sample and the optimization process performed [5, 8]. Modifications to these decision-based attacks for incorporating tabular data validity and editability constraints were made by [7].

In transferability-based attacks, the attacker trains a surrogate model, crafts an adversarial sample using a white-box attack on the surrogate model, and then utilizes the adversarial sample crafted to attack the target model in a single query [38].

An untargeted, transferability-based gradient attack designed to address tabular constraints was introduced in previous work [35, 19]. This architecture is based on NN and incorporates an embedding function to preserve feature correlations and ensure value consistency by minimizing L_2 distance and adjusting correlated features. The attack process iteratively perturbs features to reduce L_0 (i.e., the number of modified features) while applying validity and editability constraints, demonstrating its applicability in real-world scenarios. Another work [23] introduced a transferability-based attack that considers feature distribution in the perturbation process, addressing the tabular distribution challenge while excluding validity constraints.

2.2. Existing Methods for Evaluating Adversarial Attacks

Commonly used metrics for assessing the performance of adversarial attacks include:

1. **Attacker’s risk.** The attacker’s risk is assessed by the attack success rate [17, 2], the number of queries made to the target model [22, 47], and the extent to which the adversarial has been distorted, consequently becoming distinguishable. The distortion is typically measured using L_p norms such as L_0 , L_2 , and L_∞ , which quantify the magnitude of perturbations applied to the original samples [17, 27, 14, 2, 35, 19], and can also be evaluated by computing the average error

between the original sample and the corresponding adversarial samples [16].

2. **Attacker’s effort.** The attacker’s effort is assessed by the time required to create the adversarial sample, as well as the amount of data and time needed to train the surrogate model [1].

2.3. Indistinguishability in the Tabular Domain

While most of the metrics used to assess the attacker’s effort and risk are the same for tabular data domains and other domains, the risk of distinguishing an adversarial sample should be measured differently. In the computer vision domain for example, the indication for an indistinguishable adversarial sample is that the human eye is unable to recognize the difference between the adversarial sample and the original sample [46, 17, 39, 27]. It is commonly assessed by measuring the distance between the original and perturbed images using L_2 norm.

However, in the tabular domain, “human eye” inspection is less meaningful, as only domain experts can accurately examine such differences [2, 7]. Furthermore, when looking at the tabular data samples, a domain expert would “select” a limited number of features to examine and determine whether the sample is real or manipulated by an adversary [2] based on those features. Given the above, the authors proposed to evaluate the distinguishability of a tabular adversarial sample based on the number of “important” features (i.e., features that a domain expert would likely examine) altered in the adversarial attack. Accordingly, an adversarial sample is considered more perceptible as the number of changes in “important” features increases. However, this evaluation method is neither objective nor practical, as it requires a domain expert to manually assess each sample individually. Moreover, it does not consider the fact that altering even a small number of features can cause inconsistency with the rest of the sample, making it distinguishable from benign data distribution and detectable by anomaly-based methods.

Prior research highlighted the significance of both consistency [35, 23] and validity [35, 16] when analyzing the quality of adversarial samples. Validity can be assessed by examining whether each feature value falls within a valid range [2, 35] and by measuring the sample’s deviation from the distribution of benign data [35]. However, no concrete metric has been proposed to quantify the coherence and consistency of adversarial samples. The coherence and consistency of crafted samples are challenging to measure, as it is influenced by correlations between different feature values [35]. To address this gap, we propose two concrete criteria to assess the distinguishability of adversarial samples from benign samples, enabling an indirect evaluation of their coherence and consistency. We assume that adversarial samples lacking coherence or consistency with the benign data distribution are likely to exhibit anomalies, making them both distinguishable and detectable.

3. Methodological Framework for Addressing Challenges in Adversarial Attack and Evaluation within the Tabular Domain

In this section, we introduce the black-box query and transferability attacks evaluated, along with the modifications made to deal with the tabular constraints. We also present our novel technique for perturbing dependent features, as well as new criteria for evaluating the quality of adversarial attacks’ samples. These criteria focus on the distinguishability of the adversarial samples and their impact on the target model’s internal behavior within the tabular domain.

3.1. Modifying Adversarial Attacks to Address Tabular Constraints.

In our evaluation (see Section 4.5), we examine two decision-based attacks: the boundary attack [5] and the Hop-SkipJump attack [8], which were adjusted to address tabular constraints and evaluated by [7]. We implemented these attacks by additionally applying constraints based on feature distributions (e.g., limiting values according to statistical information) and making adjustments such as ensuring validity (e.g., binary or categorical constraints) and editability (guided by domain knowledge)

In addition, we performed untargeted transferability-based gradient attacks based on the architecture proposed in [35, 19], which is an advanced attack that aims to craft valid and consistent adversarial samples.

The details and pseudocode for the boundary and Hop-SkipJump attacks, as well as the transferability-based attacks, adapted to take into account the constraints of tabular data, are provided in Appendix A.

3.2. Perturbing Dependent Features.

We address the challenge of maintaining coherence and ensuring feature consistency within adversarial samples during perturbation by introducing a novel technique: for each dependent feature, we train a regression model on the benign samples. During the adversarial sample crafting process, these regression models are querying to ensure that perturbations of dependent features remain consistent with the rest of the sample. This method effectively manages both direct and indirect feature dependencies, ensuring the overall sample’s coherence and therefore less distinguishable.

In our implementation of both query- and transferability-based attacks, the attack process includes an additional step in which the dependent features, as determined by domain knowledge, are adjusted based on the regression models.

3.3. Evaluating the Quality of Adversarial Attacks

The quality of an adversarial attack can be derived from the extent to which the crafted samples maintain coherence and consistency, making them indistinguishable from benign samples. To assess this, we propose two evaluation criteria for measuring the distinguishability of adversarial samples: first, by evaluating how anomalous adversarial samples are compared to benign samples, and second, by assessing the

extent to which adversarial samples influence the internal behavior of the target model when queried.

Assessing the anomaly of the adversarial sample. To evaluate the distinguishability of adversarial samples, we propose using an anomaly detection rate metric that measures the percentage of samples identified as anomalies for each attack. This rate can be indicative of how different the adversarial samples are from the benign distribution. We calculated the anomaly detection rate using two established methods from the anomaly detection domain: *i*) the anomaly scores provided by the isolation forest method (IF) [30]; and *ii*) the reconstruction error from an autoencoder (AE) [44]. Both the anomaly score and the reconstruction error indicate the likelihood of an adversarial sample remaining coherent and consistent, and thus being indistinguishable from the original benign samples. When these values are low, the sample is considered less anomalous, and therefore less distinguishable as an adversarial sample, and vice versa.

Our proposed methodology evaluates the anomaly rate *separately* for each target class since an adversarial sample can be anomalous for the target class while still maintaining the overall distribution of the dataset — especially when the changes made to the sample are subtle, such that the sample maintains the same distribution as the original sample but is detected as anomalous when compared to the intended target class.

For each class, an anomaly detection model is trained on benign samples (i.e., the data used to train the target model). Then, based on the target model’s prediction for the adversarial sample, we query the relevant anomaly detection model with the adversarial sample. For example, if the adversarial sample was classified as ‘1’ by the target model, it would be evaluated using the anomaly detection model trained on benign samples from class 1.

In the first method, a sample is considered anomalous if the IF model identifies it as an outlier. For the second method, a sample is considered anomalous if its reconstruction error, calculated by the AE, exceeds a predefined threshold; this threshold is defined in Eq. (1):

$$Threshold(x, AE) = mean(test_{r,error}) + 0.5 * std(test_{r,error}) \quad (1)$$

where x is a data sample, AE is the autoencoder, and $test_{r,error}$ is the reconstructed error on the test set when training the AE.

The AE model consists of an embedding layer with 64 neurons, and it was trained using the Adam optimizer with a learning rate of $1e - 3$, a weight decay of $1e - 8$, for 10 epochs, and the mean square error (MSE) as the loss. The IF method, in turn, was implemented with 100 estimators, a maximum features set at one, and without bootstrapping. For comparison, the contamination parameter in the IF model was set to match the false positive rate (FPR) obtained by the AE according to the threshold defined in Eq. (1), corresponding to the proportion of benign samples with reconstruction error above this threshold.

Assessing the impact of adversarial samples on the target model.

An additional aspect of adversarial sample quality is whether they introduce inconsistency in the target model’s decision-making process. Adversarial samples can affect the target model’s decision by altering feature importance.

To quantify this impact, we developed new criteria using SHAP values [32], a widely used XAI technique that provides a unified measure of feature importance in ML models. SHAP values estimate the contribution of each feature to the prediction by comparing the actual predictions with averages across all possible feature combinations. We calculated the difference in SHAP values between benign and adversarial samples, focusing on the top-four most important features selected based on their average SHAP values computed based on the benign samples in the training dataset. The SHAP values were extracted using the SHAP TreeExplainer.

We defined two concrete metrics to evaluate this impact: *i*) the *importance-based anomaly detection rate*, which measures the percentage of adversarial samples where at least one feature’s SHAP value exceeds the maximum or falls below the minimum SHAP value for that feature in the benign dataset; and *ii*) the *average number of features with anomalous SHAP values* per sample. These metrics reflect the extent to which adversarial perturbations influenced the target model. A lower number of features with anomalous SHAP values and a reduced importance-based anomaly detection rate indicate higher quality adversarial samples, as the model’s internal behavior remains more consistent despite changes in predictions.

In addition to serving as a metric assessing the quality of adversarial samples, the anomaly detection rate metrics, whether computed on adversarial samples or SHAP values, can serve as the basis of a defense mechanism, as they are strong indicator of attacked samples.

4. Experimental Setup

4.1. Research Questions

In this study, we address the following research questions regarding the tabular domain:

- **RQ#1** To what extent do query-based attacks reflect the behavior of transferability-based gradient attacks?
- **RQ#2** How the perturbed samples of different attacks’ strategies differ in terms of the attacker’s risk and effort?
- **RQ#3** Is the model’s decision-making process aligned according to the samples’ SHAP values for both a benign samples and perturbed samples?

4.2. Datasets

We conducted our evaluation on two publicly available, real-life tabular datasets and an additional proprietary tabular dataset. These datasets contain a relatively large number of samples and features, as well as a variety of feature types, to ensure robust and reliable results.

1. *The Hateful Users on Twitter (Hate) dataset* [43]. This dataset contains 4,971 records of English-speaking Twitter users that were manually annotated as hateful or non-hateful users. This dataset is unbalanced and includes 544 records from class 1 (i.e., hateful users). The dataset comprises 115 numerical and categorical features, with 109 of them being mutable (i.e., can be changed by the attacker).
2. *Intensive Care Unit (ICU) dataset*¹ [20]. This dataset, which contains the medical records of 83,978 patients who were admitted to the intensive care unit, is used to predict the mortality of the patients. The dataset is unbalanced and includes 7,915 records from class 1 (i.e., patients who died while in the ICU). The dataset comprises 74 numerical and categorical features, 45 of which are mutable and five of which contain values that are dependent on other features.
3. *Video Transmission Quality (VideoTQ) dataset*. This proprietary commercial dataset was obtained from RADCOM², a company specializing in service assurance for telecom operators, and it contains records of 54,825 streaming service media broadcasts. This dataset is used to predict a transmission’s resolution (i.e., high or low resolution). The dataset is unbalanced and includes 10,000 records from class 1 (i.e., high resolution). The dataset comprises 23 numerical and categorical features, nine of which are mutable.

4.3. Dataset Preprocessing

The preprocessing performed on each dataset (illustrated in Fig. 1 (b)) differs according to its characteristics, with the aim of creating highly accurate target models that are based on multiple features’ importance in the model’s decision-making process.

Hate dataset. In the preprocessing performed on the Hate dataset, we followed the preprocessing methodology outlined by Kaggle³. We also performed additional preprocessing steps, including removing the ‘*user_id*’ feature, systematically eliminating outliers, dropping features with a correlation exceeding 90%, and excluding instances with more than 80% missing data. In addition, features for which over 75% of the values were the same were removed.

We also performed label encoding on the binary and categorical features and filled in missing values by employing a regression model to predict the values for each feature. Additionally, features that contain the GloVe representations [40] of other features (which include ‘*glove*’ in their names) were removed, resulting in a distilled set of 311 features. To ensure that only meaningful and important features were used, we trained four models on the dataset (XGBoost [9], GradientBoost [15], LightGBM [25], and random forest [4]) and selected the top-40 important features for each model;

the importance of all of these features exceeded 0.0001. The resulting dataset contains 115 features and 4,971 samples.

ICU dataset. In the preprocessing performed on the ICU dataset, we followed the preprocessing methodology outlined by Kaggle⁴. We also performed additional preprocessing, removing outliers, eliminating highly correlated features (with over 90% correlation), and excluding instances with over 80% missing values. In addition, features for which over 75% of the values were the same were removed. Samples for which the ‘*bmi*’ feature was missing, values were filled in by using the BMI formula based on the values in the ‘*height*’ and ‘*weight*’ features. For other features, we filled in missing values by using a regression model to predict the values for each feature. Categorical features were label-encoded, and missing values were filled in by using the median feature value.

VideoTQ dataset. In the preprocessing performed on the VideoTQ dataset, we removed 15 records that had missing values, and eliminated outliers and highly correlated features (with over 90% correlation). Categorical features were label-encoded, and all timestamps were converted into separate date and time formats.

For all datasets, the editable and immutable features were determined and selected by a domain expert. All datasets were split into training and test sets, with 75% of the samples serving as the training set. Oversampling was performed by duplicating the training set samples in class 1 to address the significant class imbalance in the datasets. The oversampled training set was split into a target training set and a surrogate training set (for the attacker’s use in the transferability-based attacks). The test set is also used to create adversarial samples (i.e., the attack set) as illustrated in Fig. 1 (c) and further detailed in Section 4.8.

4.4. Target Models

For our evaluation, we trained four different ML target models: XGBoost [9] (XGB), GradientBoost [15] (GB), LightGBM [25] (LGB), and random forest [4] (RF) (see 1 (d)). The hyperparameters used to train the models were fine-tuned, and therefore varied across different training sets. The XGBoost target models were trained using 90, 70, and 300 estimators; a max depth of 3, 8, and 5; and a learning rate of 1, 0.1, and 1 for the Hate, ICU, and VideoTQ datasets respectively. The GradientBoost target models were trained using 40, 500, and 300 estimators; a max depth of 7, 6, and 5; and a learning rate of 2.5, 0.01, and 1 for the Hate, ICU, and VideoTQ datasets respectively. The LightGBM target models were trained using 300, 200, and 200 estimators; a max depth of 7, 8, and 8; and a learning rate of 1, 0.1, and 0.1 for the Hate, ICU, and VideoTQ datasets respectively. The random forest target models were trained using 100, 500, and 500 estimators and a max depth of 4, 9, and 9 for the Hate, ICU, and VideoTQ datasets respectively.

¹ICU:kaggle.com/competitions/widsdatathon2020/data

²radcom.com/

³kaggle.com/code/binaicrai/fork-of-fork-of-wids-lgbm-gs

⁴kaggle.com/code/binaicrai/fork-of-fork-of-wids-lgbm-gs

4.5. Attack Configuration

In our comparison of different types of attacks, we used two query-based attacks and five transferability-based gradient attacks that varied in terms of their feature selection techniques. The boundary attack was used with an epsilon of one, a delta of one, maximal iterations of 3000, the number of trials set at 20, and an adaptation step of one. The HopSkipJump attack was used with the L2 norm, maximal iterations of 50, the max-eval parameter set at 10000, the init-eval set at 500, and an init size of 100. The parameters of the boundary and HopSkipJump attacks were identical for all datasets, except for the maximal iteration number; for the VideoTQ dataset this was set at 1000 in the HopSkipJump attack.

The transferability-based attacks require the attacker to train a surrogate model (illustrated in Fig. 1 (d, e)). In our evaluation, all surrogate models were NNs, and we used an embedding layer to try to maintain the consistency of the crafted samples, following the approach employed in other studies [35, 19]. All surrogate models were comprised of two components: a sub-model for embedding and a sub-model for classification, both of which were fine-tuned for optimized performance. The embedding sub-model had an input size matching the number of features in the input sample, followed by a dense layer with 256 neurons, and ReLU and PReLU activations for the Hate and VideoTQ datasets respectively. For the ICU dataset, the embedding sub-model had three dense layers with 256, 128, and 64 neurons and ReLU activation for all layers. The output size of all embedding sub-models was set at 16, i.e., the embedding size. The classification sub-model had a dense layer with 16 neurons (matching the embedding size) with ReLU activation for the Hate and ICU datasets, and PReLU activation for the VideoTQ datasets. This was followed by a dropout layer with a dropout rate of 0.1. All surrogate models were trained using the binary cross-entropy loss function [31] and the Adam optimizer [26] with a learning rate of 0.2 for the Hate and VideoTQ datasets, and 0.1 for the ICU dataset.

After training the surrogate models, the attacker selects k features and identifies the n features most correlated with them, which are then perturbed during each attack iteration. Each transferability-based attack uses a different selection technique to determine which features to perturb (see Appendix A). In attacks employing importance-based selection techniques, features are selected based on their importance as determined by XGBoost, GradientBoost, LightGBM, and Random Forest models, trained separately for these attacks. For all attacks, n was set at one, and the correlated features were selected by using Pearson’s correlation coefficient [48], where k was set at two;

4.6. Regression Models

Of the datasets used in our evaluation, the ICU dataset is the only one containing dependent features where their dependencies are not well-defined. Specifically, these dependent features are: ‘*apache_3j_bodysystem*,’

‘*apache_3j_diagnosis*,’ ‘*d1_mbp_invasive_max*,’ and ‘*d1_mbp_invasive_min*.’

The regression models were trained on the dataset used to train the surrogate models, using 200 estimators, a max depth of six, and a learning rate of 0.1 for the ‘*apache_3j_bodysystem*’ and ‘*apache_3j_diagnosis*’ features, and 0.01 for the ‘*d1_mbp_invasive_max*’ and ‘*d1_mbp_invasive_min*’ features.

4.7. Threat Model

We assume that the attacker can query the target model and has a query budget of one for transferability-based attacks and an unlimited query budget for query-based attacks; in each query to the target model, the attacker obtains the confidence score of the prediction. In addition, we assume that the attacker has no prior knowledge about the specific model architecture or the ML algorithm used. The attacker also has no access to the internal parameters of the model (such as weights and biases) and cannot calculate any gradients related to the model. Furthermore, the attacker does not have access to the target model’s training data; However, we assume that the attacker has a surrogate dataset derived from the same distribution, meaning that it contains the same features, in the same order, as the training data.

4.8. Evaluation Setup

For a robust evaluation, we filtered the test set by selecting only samples correctly classified by both the target and surrogate models, excluding those already misclassified, retaining 85%, 69%, and 91% of samples from the Hate, ICU, and VideoTQ datasets respectively. In addition, to properly evaluate each attack, we randomly selected a balanced number of samples from each class, which were then used as the attack set. This resulted in attack sets that contained 182, 1000, and 1000 samples for the Hate, ICU, and VideoTQ datasets respectively. In the evaluation of each adversarial attack’s samples, only those samples that successfully misled both the surrogate and target models (or only the target model in the case of a query-based attack) were used.

4.9. Evaluation Metrics

The main objective of our evaluation is to analyze the characteristics of and differences between black-box query- and transferability-based adversarial attacks with respect to three key factors: the attacker’s risk, the attacker’s effort, and the attacks’ quality (illustrated in Fig. 1(f)). To perform a thorough analysis, we used the evaluation metrics commonly used in the literature and the metrics proposed in this work.

To assess the **attacker’s risk** we used three metrics (illustrated in Fig. 1(f-1)): *i*) the percentage of samples that successfully misled the model (attack *success rate*); *ii*) the average number of modified features (L_0) which might influence the attack’s ability to be successfully performed in real-life tabular data domains (due to the possible cost of changing the features), and the average Euclidean distance between the original and adversarial samples (L_2); and *iii*) the average number of queries required.

Table 1

Target and surrogate models’ performance on the test set.

Dataset	Metric	Models				
		GB	LGB	XGB	RF	Surrogate
Hate	Accuracy	0.91	0.92	0.88	0.91	0.95
	F1 Score	0.91	0.92	0.87	0.91	0.95
	Precision	0.93	0.94	0.94	0.89	0.92
	Recall	0.89	0.91	0.82	0.92	1.00
ICU	Accuracy	0.80	0.80	0.77	0.78	0.78
	F1 Score	0.79	0.81	0.75	0.77	0.79
	Precision	0.82	0.84	0.82	0.81	0.81
	Recall	0.77	0.74	0.69	0.74	0.74
VideoTQ	Accuracy	0.98	0.99	0.98	0.98	0.96
	F1 Score	0.99	1.00	0.99	0.99	0.97
	Precision	0.91	0.97	0.96	0.93	0.86
	Recall	0.98	0.99	0.96	0.98	0.93

To assess the **attacker’s effort** we used three metrics (illustrated in Fig. 1(f-2)): *i*) the time it took to craft an adversarial sample; *ii*) the number of data samples needed to execute the attack; and *iii*) the memory resources and computing capabilities required to craft the adversarial sample and perform the optimization process.

The **attacks’ quality** is reflected in the crafted adversarial sample, which were assessed using three metrics (illustrated in Fig. 1(f-3)): *i*) the *anomaly detection rate* of adversarial samples compared to benign samples, using IF and AE models, where a higher rate indicates less consistency and coherence; *ii*) the percentage of samples with at least one feature with an anomalous SHAP value (*importance-based anomaly detection rate*); and *iii*) the average number of features with anomalous SHAP values per sample.

In all three metrics, a lower number is better as higher values indicates an abnormal influence on the model’s decision-making process. Each experiment was conducted separately for each target model, as SHAP values vary across models.

4.10. Experimental Environment Setup

All experiments were performed on an Intel Core i7-10700 CPU at 2.90 GHz processor with the Windows 10 Pro operating system, an Intel UHD Graphics 630 graphics card, and 32 GB of memory. The code used in the experiments was written using Python 3.10.9 and the following Python packages: PyTorch 2.0.0, adversarial-robustness-toolbox 1.13.0 [37], pandas 1.5.2, NumPy 1.23.5, TensorFlow 2.10.0, and Keras 2.10.0.

5. Experimental Results

5.1. Models’ Performance

Table 1 summarizes the performance of all target and surrogate models examined, presenting the accuracy, F1 score, precision, and recall values obtained by each model on the test set. As can be seen, all models were high-performing. The target models for the Hate dataset obtained accuracy

values ranging from [88% – 91%], F1 scores ranging from [87% – 92%], precision values ranging from [89% – 94%], and recall values ranging from [82% – 92%]. The target models for the ICU dataset obtained accuracy values ranging from [77% – 80%], F1 scores ranging from [75% – 81%], precision values ranging from [81%–84%], and recall values ranging from [69%-77%]. The target models for the VideoTQ dataset obtained accuracy values ranging from [98% – 99%], F1 scores ranging from [99% – 100%], precision values ranging from [91% – 97%], and recall values ranging from [96%-99%].

5.2. Attacker’s Risk

Tables 2 and 3 and Fig. 2 present the results for the attacker’s risk metrics (see Section 4.9) for the query- and transferability-based attacks performed against different target models on each dataset.

Table 2 provides details on the attack’s success rate (SR) on the target model, the attack’s success rate on the surrogate model (Surrogate SR), the transfer success rate from the surrogate model to the target model (Transfer SR), and the overall success rate (Overall SR), which represents the percentage of adversarial samples that successfully mislead both the surrogate model and the target model.

As detailed in Table 2, the query-based attacks have consistently high success rates (SR) on all target models across the Hate and ICU datasets. For example, on the Hate and ICU datasets, both attacks achieve success rates ranging between [98% – 100%] across all target models. In comparison, the success rate varies more for the transferability-based attacks. The success of these attacks relies on the performance of the surrogate models and the transferability of adversarial samples. For instance, on the Hate dataset, despite successfully fooling surrogate models in 98.9% of cases, the transferability-based attacks demonstrated limited effect on the target models, with success rates falling below 12% when employing random feature selection (Transfer random). However, when using importance-based feature selection (Transfer imp.), the success rates improved, ranging between [20% – 86%]. A similar phenomenon can be observed on the ICU dataset, where transferability-based attacks continued to perform variably, depending on the feature selection method employed. On the VideoTQ dataset, unlike the other datasets, transferability-based attacks had more consistent performance, achieving a ~50% success rate overall. In contrast, the query-based attacks displayed more variability, with success rates ranging between [65.9% – 82.6%] for the boundary attack and between [50% – 67.9%] for the HopSkipJump attack.

Table 3 presents the average number of queries required to generate adversarial samples for query-based attacks. As can be seen, the examined query-based attacks require a significant number of queries, ranging from hundreds to hundreds of thousands. In contrast, transferability-based attacks require just a single query for all datasets.

Table 2

Attacker’s risk: performance of query- and transferability-based attacks on different target models, including the attack’s success rate (SR) on the target model, the attack’s success rate on the surrogate model (*Surrogate SR*), the transfer success rate from the surrogate model to the target model (*Transfer SR*), and the overall success rate (*Overall SR*), which represents the percentage of adversarial samples that successfully mislead both the surrogate model and the target model (imp. refers to an importance-based feature selection technique).

Dataset	Target Model	Query Attacks			Transferability Attacks			
		boundary	HopSkipJump SR (%)	random	GB imp. Surrogate SR (%) / Transfer SR (%) / Overall SR (%)	LGB imp. Surrogate SR (%) / Transfer SR (%) / Overall SR (%)	XGB imp. Surrogate SR (%) / Transfer SR (%) / Overall SR (%)	RF imp. Surrogate SR (%) / Transfer SR (%) / Overall SR (%)
Hate	GB	100	100	98.9 / 13.9 / 13.7	98.9 / 70.6 / 69.8	98.9 / 44.4 / 44.0	98.9 / 83.3 / 82.4	98.9 / 86.7 / 85.7
	LGB	100	100	98.9 / 7.8 / 7.7	98.9 / 71.1 / 70.3	98.9 / 45.6 / 45.1	98.9 / 73.9 / 73.1	98.9 / 85.0 / 84.1
	XGB	100	100	98.9 / 12.2 / 12.1	98.9 / 70.0 / 69.2	98.9 / 36.7 / 36.3	98.9 / 68.3 / 67.6	98.9 / 71.7 / 70.9
	RF	100	100	98.9 / 2.8 / 2.7	98.9 / 36.7 / 36.3	98.9 / 20.6 / 20.3	98.9 / 54.4 / 53.8	98.9 / 73.3 / 72.5
ICU	GB	98.6	98	87.4 / 9.4 / 8.2	87.8 / 45.4 / 39.9	87.4 / 25.4 / 22.2	88.6 / 41.9 / 37.1	88.4 / 45.8 / 40.5
	LGB	98.7	97.9	87.4 / 12.8 / 11.2	87.8 / 35.8 / 31.4	87.4 / 29.1 / 25.4	88.6 / 34.2 / 30.3	88.4 / 36.4 / 32.2
	XGB	99.9	98.2	87.4 / 24.5 / 21.4	87.8 / 55.2 / 48.5	87.4 / 41.3 / 36.1	88.6 / 50.5 / 44.7	88.4 / 55.3 / 48.9
	LGB	99.2	99.2	87.4 / 11.4 / 10.0	87.8 / 44.9 / 39.4	87.4 / 18.4 / 16.1	88.6 / 42.8 / 37.9	88.4 / 45.4 / 40.1
VideoTQ	GB	82.6	57.6	67.6 / 73.7 / 49.8	67.6 / 74.4 / 50.3	67.6 / 74.3 / 50.2	67.6 / 73.5 / 49.7	67.6 / 73.7 / 49.8
	LGB	73.7	53	67.6 / 74.1 / 50.1	67.6 / 74.7 / 50.5	67.6 / 74.9 / 50.6	67.6 / 73.4 / 49.6	67.6 / 74.0 / 50.0
	XGB	81.7	67.9	67.6 / 74.1 / 50.1	67.6 / 74.3 / 50.2	67.6 / 74.1 / 50.1	67.6 / 73.2 / 49.5	67.6 / 73.8 / 49.9
	RF	65.9	50	67.6 / 74.0 / 50.0	67.6 / 74.0 / 50.0	67.6 / 74.0 / 50.0	67.6 / 74.0 / 50.0	67.6 / 74.0 / 50.0

Table 3

Attacker’s risk: average number of *queries* required to execute query-based attacks.

Dataset	Attack	Target Model			
		GB	LGB	XGB	RF
Hate	Boundary	292.5	302.0	275.4	309.8
	HopSkipJump	120260.0	120246.6	120243.4	120361.2
ICU	Boundary	902.3	2909.9	910.9	3531.7
	HopSkipJump	119231.3	119402.4	119642.7	121632.6
VideoTQ	Boundary	59604.1	57627.6	58860.6	60173.1
	HopSkipJump	16310.9	118374.4	103314.8	108680.1

Fig. 2 illustrates the distribution of both the number of modified features (L_0) and the Euclidean distance (L_2) between the adversarial attacks and the original samples.

As can be seen in the figure, for most target models on the Hate and ICU datasets the examined query-based attacks consistently require more feature changes (i.e., larger L_0 distances) than the transferability-based attacks. For instance, on the Hate dataset transferability-based attacks modify approximately 7 features, whereas query-based attacks modify around 103.

However, the VideoTQ dataset exhibits a less consistent pattern, with the boundary attack shows substantial variation in L_0 values, including samples with considerably lower L_0 distances than those of transferability-based attacks. This suggests that, in some cases, attacks required more feature modifications to succeed on this dataset.

In terms of L_2 distance, the two query-based attacks differ. Across the Hate and ICU datasets, the boundary attack generally causes larger distortions compared to transferability-based attacks. However, the VideoTQ dataset exhibits a different pattern: the boundary attack achieves notably lower L_2 distances on the GB and XGB target models than the transferability-based attacks. In contrast,

while the HopSkipJump attack typically outperforms most transferability-based attacks by achieving lower median L_2 distances on most target models, it performs less effectively on the VideoTQ dataset, showing higher median L_2 distances on several target models.

In conclusion, while query-based attacks tend to achieve higher attack success rates, they have higher operational costs due to the large number of queries required. On the other hand, transferability-based attacks, despite their lower success rates on the target models, present a lower risk in terms of query overhead and perturbation efficiency, as demonstrated by their reduced L_0 and L_2 distances, especially when feature-importance-based selection is applied.

5.3. Attacker’s Effort

To assess the attacker’s effort, we compared the performance of the query- and transferability-based attacks in terms of the computational time, the required amount of data, and the computational resources needed (see Section 4.9).

With respect to the *computational time*, the attacker’s objective is to minimize the amount of time it takes to craft an adversarial sample. In query-based attacks, the computational time includes: *i*) the time it takes to query the target model (denoted as α); and *ii*) the time it takes to perform a single optimization iteration (denoted as β). The total amount of time it takes to craft an adversarial sample is calculated in Eq. (2):

$$Time(x, M) = nt^2\alpha\beta \quad (2)$$

where x is a data sample, M is the target model, n is the number of queries required to craft a successful adversarial sample, and t is the time it takes to perform a single query. When considering solely the query-related aspects of the required time, query-based attacks are at a disadvantage compared to transferability-based attacks, since many more

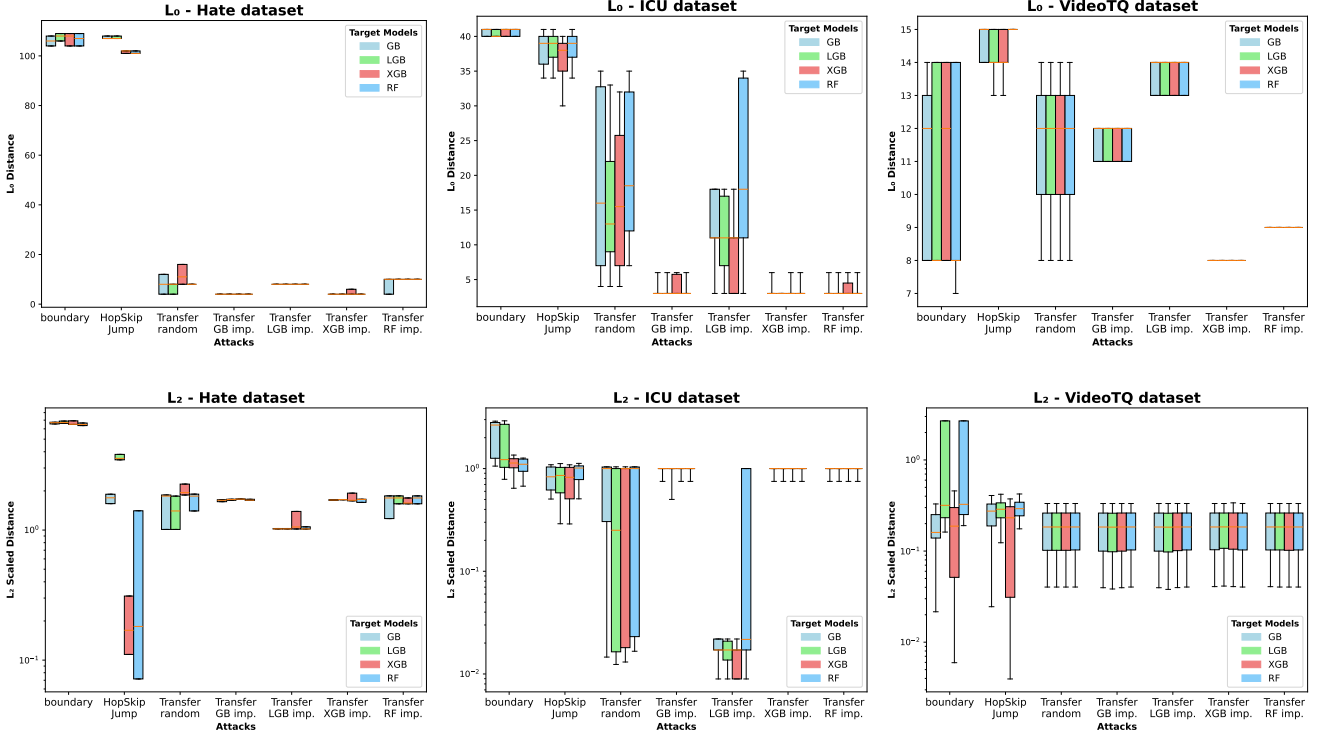


Figure 2: Attacker’s risk: number of changed features (L_0 distance) and distortion size (L_2 distance), across query- and transferability-based attacks.

queries to the target model are required (see Section 5.2). However, in transferability-based attacks, there is another aspect to consider – the surrogate model’s training and querying time. The total amount of time it takes to craft an adversarial sample is calculated in Eq. (3), where we assume that the time it takes to perform a query to the target model is identical to the time required to perform a query to the surrogate model.

$$Time(x, M) = m t^2 \alpha \beta + T_{surrogate} + t \quad (3)$$

where x is a data sample, M is the target model, m is the number of queries to the surrogate model required to craft a successful adversarial sample, and $T_{surrogate}$ is the time it takes to train the surrogate model. In transferability-based attacks that rely on an additional feature importance model, the total time must also include the time it takes to train that model.

In our evaluation, we found that the total amount of time it took to produce a single adversarial sample in query-based attacks was, on average, 518.4 seconds. However, in transferability-based attacks, it was ~ 243.5673 seconds: ~ 240.49 seconds to train the surrogate and feature importance models, 0.0773 seconds to generate the sample w the surrogate model, and ~ 3 seconds to query the target model. Based on this, we can conclude that although transferability-based attacks require training additional models, the total computational time required to craft a single adversarial sample is shorter than in query-based attacks.

With respect to the *amount of data* required, the attacker’s objective is to minimize the amount of data. In query-based attacks, the only data required by the attacker is the original sample that the adversarial sample will be based on, however in transferability-based attacks, the attacker must also possess a surrogate dataset to train the surrogate and feature importance models.

Based on this, we can conclude that transferability-based attacks require more data samples than query-based attacks.

In our evaluation, the surrogate model was trained with the exact same amount of data used to train the target models (3,320, 62,848, and 33,727 samples from the Hate, ICU, and VideoTQ datasets respectively), and achieved satisfactory performance.

With respect to *computational resources*, the attacker’s objective is to minimize the amount of computational resources needed. In query-based attacks, the required resources include computational power for the adversarial sample generation process and storage to store the original and adversarial samples and the byproducts of the process (e.g., the target model’s response), which can be substantial when dealing with a large number of queries. In contrast, transferability-based attacks require the resources mentioned above, as well as additional storage and computational resources to train and store the surrogate and feature importance models. Based on this, we can conclude that transferability-based attacks require more computational resources than query-based attacks.

In conclusion, while query-based attacks require less data, transferability-based attacks require less computational time and resources. However, they are limited by lower success rates compared to query-based attacks, as discussed in Section 5.2.

5.4. Attack’s Quality

In our evaluation, we assessed query- and transferability-based attacks in terms of the quality of the adversarial samples produced. This quality can be examined by considering both the adversarial sample’s coherence and its impact on the target model’s decision-making process. To measure the coherence of adversarial samples, we propose using metrics based on AE and IF models. To evaluate the impact on the target model’s decision-making process, we introduced two new metrics derived from the SHAP framework (see Section 4.9).

Coherence of the adversarial sample. Fig. 3 presents the anomaly detection rates derived from the values obtained using the IF model and the reconstruction errors from the AE for adversarial samples for each evaluated attack, target class, and dataset. Each anomaly detection rate represents the percentage of adversarial samples identified as anomalies. For the AE, a sample is considered anomalous if its reconstruction error exceeds a predefined threshold (see Eq. (1)). The false positive rate (FPR) for benign samples, based on the specified threshold, is 0.020 and 0.011 for class 0 and class 1 on the Hate dataset, 0.038 and 0.038 on the ICU dataset, and 0.014 and 0.002 on the VideoTQ dataset. The same FPR was applied to the IF model for comparison.

On the Hate dataset, the boundary attack led to a 100% detection rate for adversarial samples for both target classes for both the AE and IF models. For the HopSkipJump attack, a 100% anomaly detection was obtained for adversarial samples in class 0 by both the AE and IF models when targeting the GB and LGB models; however, no anomalies were detected for adversarial samples in class 1 across all target models. This discrepancy may arise from HopSkipJump’s initial adversarial sample selection and the optimization process, i.e., selecting a sample from the target class that is closest to the original sample and increasing proximity to the original sample using gradient estimation, whereas the boundary attack uses a random initial adversarial sample from the target class and does not employ gradient estimation (see Appendix A). In the case of the transferability-based attacks, only the AE successfully detected anomalies, achieving a 100% anomaly detection rate for most attacks for both target classes.

On the ICU dataset, the boundary attack demonstrated similar performance trends as observed for the Hate dataset, however, the HopSkipJump attack resulted in fewer detected anomalies for both target classes across both the AE and IF models. The transferability-based attacks also led to significantly fewer anomalies, with the exception of the LGB importance-based (LGB imp.) and random-based selection attacks. These two methods resulted in 60–90% of samples

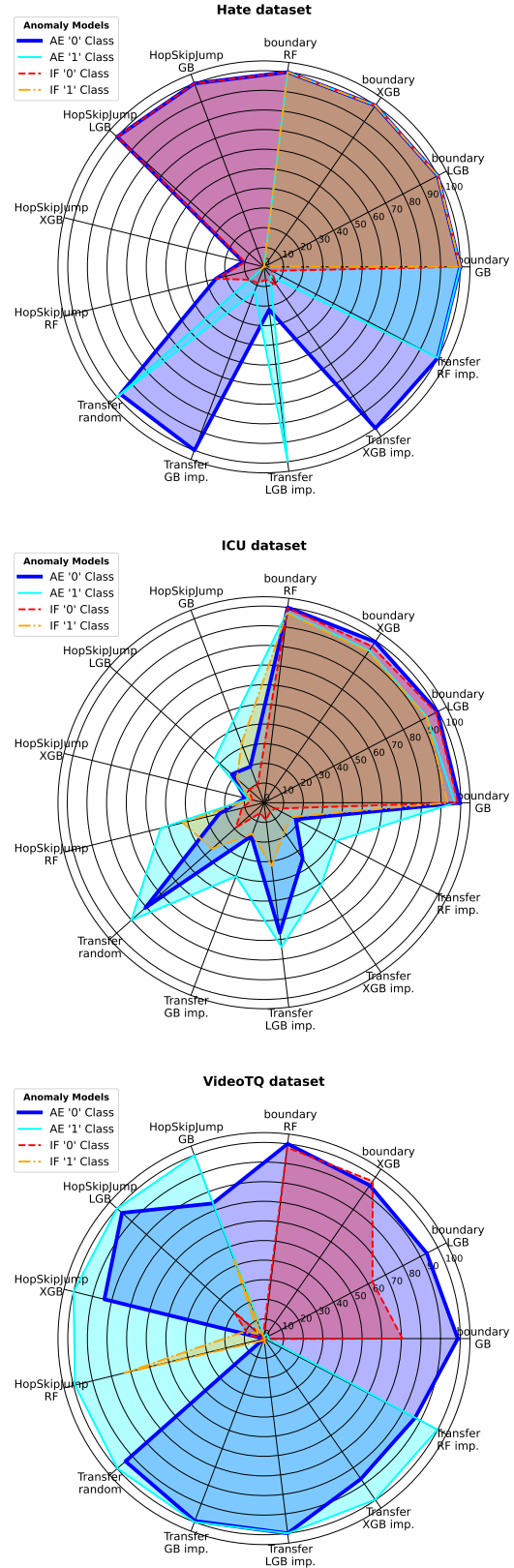


Figure 3: Attacks’ quality evaluated based on the *anomaly detection rate* by AE and IF models across datasets, computed separately for each class. The FPR on all datasets for both classes is less than 0.04.

Table 4

Attacks’ quality: results based on the *importance-based anomaly detection rate* (percentage of samples with at least one feature with an anomalous SHAP value) and the *average number of anomalous features* computed based on their SHAP values. **Bold** values highlight samples with the fewest changes in SHAP values, indicating high-quality samples in terms of having minimal impact on the target model’s decision process.

Dataset	Target Model	Query Attacks			Transferability Attacks			
		boundary	HopSkipJump	random	GB imp.	LGB imp.	XGB imp.	RF imp.
		Importance-based Anomaly Detection Rate (%) / Avg. Number of Anomalous Features per Sample						
Hate	GB	100.0 / 17.9	100.0 / 16.2	100.0 / 23.4	100.0 / 22.4	81.2 / 8.6	32.7 / 0.7	44.9 / 1.2
	LGB	69.8 / 1.8	65.9 / 2.0	92.9 / 4.1	98.4 / 4.4	95.1 / 3.0	71.4 / 1.4	53.6 / 0.9
	XGB	45.1 / 0.9	35.7 / 0.5	100.0 / 6.6	100.0 / 6.2	80.3 / 3.2	13.8 / 0.2	36.4 / 0.5
	RF	85.2 / 2.1	87.4 / 1.8	100.0 / 8.6	100.0 / 9.2	78.4 / 6.0	64.3 / 1.2	68.9 / 1.4
ICU	GB	83.9 / 1.9	74.9 / 1.6	80.5 / 1.3	71.4 / 1.3	14.0 / 0.2	17.3 / 0.2	20.7 / 0.3
	LGB	17.1 / 0.2	25.9 / 0.3	77.7 / 1.6	67.8 / 1.4	22.4 / 0.3	31.4 / 0.4	24.8 / 0.3
	XGB	23.3 / 0.3	23.0 / 0.3	48.1 / 0.7	46.2 / 0.6	16.3 / 0.2	15.9 / 0.2	14.9 / 0.2
	RF	10.5 / 0.1	9.8 / 0.1	9.0 / 0.1	10.2 / 0.1	11.2 / 0.1	10.3 / 0.1	12.0 / 0.1
VideoTQ	GB	24.1 / 0.3	11.8 / 0.6	1.2 / 0.0	2.6 / 0.1	66.7 / 2.7	100.0 / 4.0	71.5 / 3.2
	LGB	29.0 / 0.3	28.9 / 0.3	1.8 / 0.0	2.0 / 0.0	4.3 / 0.0	10.3 / 0.1	7.4 / 0.1
	XGB	70.9 / 1.6	71.7 / 1.1	12.6 / 0.1	13.3 / 0.2	49.3 / 0.6	80.6 / 1.3	62.7 / 0.9
	RF	73.7 / 1.3	95.2 / 1.7	1.8 / 0.0	2.0 / 0.0	41.2 / 0.4	92.2 / 1.3	93.4 / 1.5

from both target classes being detected as anomalies by the AE model.

On the VideoTQ dataset, all attacks resulted in high anomaly detection rates (85–100%) by the AE model. Except for the boundary attack, which achieved a 0% anomaly detection rate for class 1 by both the AE and IF models.

As shown in Fig. 3, the two query-based attacks demonstrate distinct behaviors in terms of the models’ anomaly detection rates. Most adversarial samples generated by the boundary attack were detected as anomalous by both models. In contrast, adversarial samples from the HopSkipJump attack, similar to those from transferability-based attacks, were consistently detected as anomalous only by the AE model.

Notably, despite the HopSkipJump and transferability-based attacks producing samples with lower L_2 distances (as detailed in Section 5.2, these samples were still identifiable as anomalous. This suggests that even subtle perturbations introduced by these attacks can still be identified as anomalous.

Impact on the target model’s decision-making process.

Figs. 4 to 6 presents the distribution of SHAP values for adversarial versus benign samples across different attacks and datasets for each target model. To simplify the presentation, we focus on the top-four most important features, selected based on their average SHAP values computed on the benign training dataset.

As shown in the figures, for most target models and datasets, there is at least one feature where the SHAP value distribution across attacks varies significantly. Analyzing the SHAP-based feature importance of a queried sample can therefore be an effective technique for identifying attacks.

Table 4 presents the results in terms of the proposed concrete metrics that utilize SHAP values to assess the quality

of adversarial samples. For each attack and target model, the table shows the percentage of samples with at least one anomalous feature based on SHAP values (importance-based anomaly detection rate) and the average number of anomalous features per sample (as described in Section 4.9). Lower values indicate that the target model’s decision-making process was less affected (i.e., the model relies on similar features for prediction).

The boundary attack demonstrated high importance-based anomaly detection rates across most datasets and models, particularly on the Hate dataset, where it reached 100% across all target models except XGB (45.1%). This suggests that the Boundary attack tends to generate adversarial samples with significant changes in feature importance. The HopSkipJump attack showed variable performance, with high importance-based anomaly detection rates (e.g., 100% for the GB model on the Hate dataset) but lower rates on models such as the RF model on the ICU dataset (9.8%) and the GB model on the VideoTQ dataset (11.8%). This variability indicates that the attack’s influence on feature importance is inconsistent across models and datasets.

In general, transferability-based attacks tend to result in lower importance-based anomaly detection rates and fewer anomalous features compared to query-based attacks, indicating less distinguishable changes to feature importance. An exception to this is the random attack on the Hate and ICU datasets (100% and 80% respectively), as well as the GB importance- and LGB importance-based selection attacks (abbreviated as GB imp. and LGB imp.) on the Hate dataset, which resulted in higher importance-based anomaly detection rates (e.g., 95.1% for LGB imp. attack). However, the number of anomalous features in these cases remained relatively low, which can be explained by the fewer

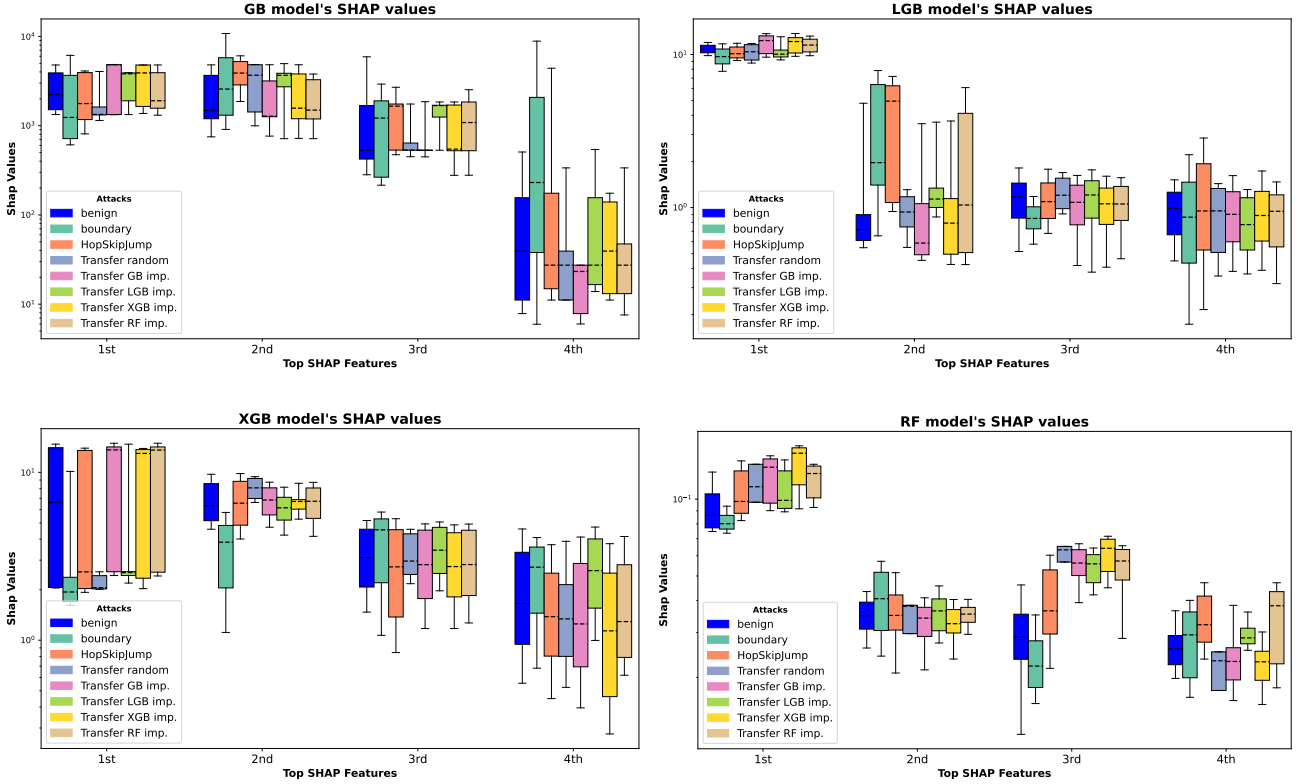


Figure 4: Attacks' quality evaluated based on the impact on the target model's decision-making process; SHAP value distribution for benign (blue) and adversarial samples (on the **Hate dataset**), across the top-four most important features selected based on their average SHAP values computed on the benign training dataset.

perturbed features, as indicated by the L_0 results (see Section 5.2). On the ICU dataset, transferability-based attacks also resulted in lower importance-based anomaly detection rates compared to query-based attacks, with the exception of GB imp. (71.4% importance-based anomaly detection rate). This suggests that transferability-based attacks might be less disruptive in medical datasets.

The VideoTQ dataset presented mixed results, with relatively high importance-based anomaly detection rate for the XGB imp. and RF imp. attacks (up to 93.4% for XGB imp. and 100% for RF imp.), indicating variability in how transferability-based attacks affect SHAP values in communication-based datasets.

When computing the average number of anomalous features per sample, query-based attacks tend to result in a higher number of anomalous features, impacting more features across all datasets. Transferability-based attacks generally led to fewer anomalous features per sample, with the exception of the random attack, emphasizing their subtler impact on the model's internal decision-making process.

Based on the results in Table 4, we conclude that transferability-based attacks generally produce smaller differences between the SHAP representations for benign and adversarial samples, indicating higher-quality samples with fewer anomalies and consequently, less impact on the target model's decision-making process. However, in some

instances, these anomalies are still detectable. In contrast, query-based attacks, particularly the examined Boundary and HopSkipJump attacks, significantly alter SHAP values, resulting in higher importance-based anomaly detection rates and a larger number of affected features, leading to a more pronounced impact on model behavior. Overall, SHAP-based anomaly detection proves to be an effective method for identifying adversarial samples. These findings highlight the importance of considering both the number of anomalous features and the anomaly detection rates – based on both sample values and feature importance – when assessing the impact of adversarial attacks on model robustness.

6. Discussion

The results from our evaluation of the attacker's risk highlight the trade-offs between different attacks' strategies. The examined query-based attacks, which are boundary and HopSkipJump attacks, achieved near-perfect success rates, often exceeding 98% across all target models. However, this high consistency comes at the cost of larger distortion that is reflected in increased L_0 and L_2 distances. They are also computationally expensive due to the high volume of queries required. In contrast, the examined transferability-based attacks modified fewer features and resulted in subtle distortions, making them more efficient in terms of query

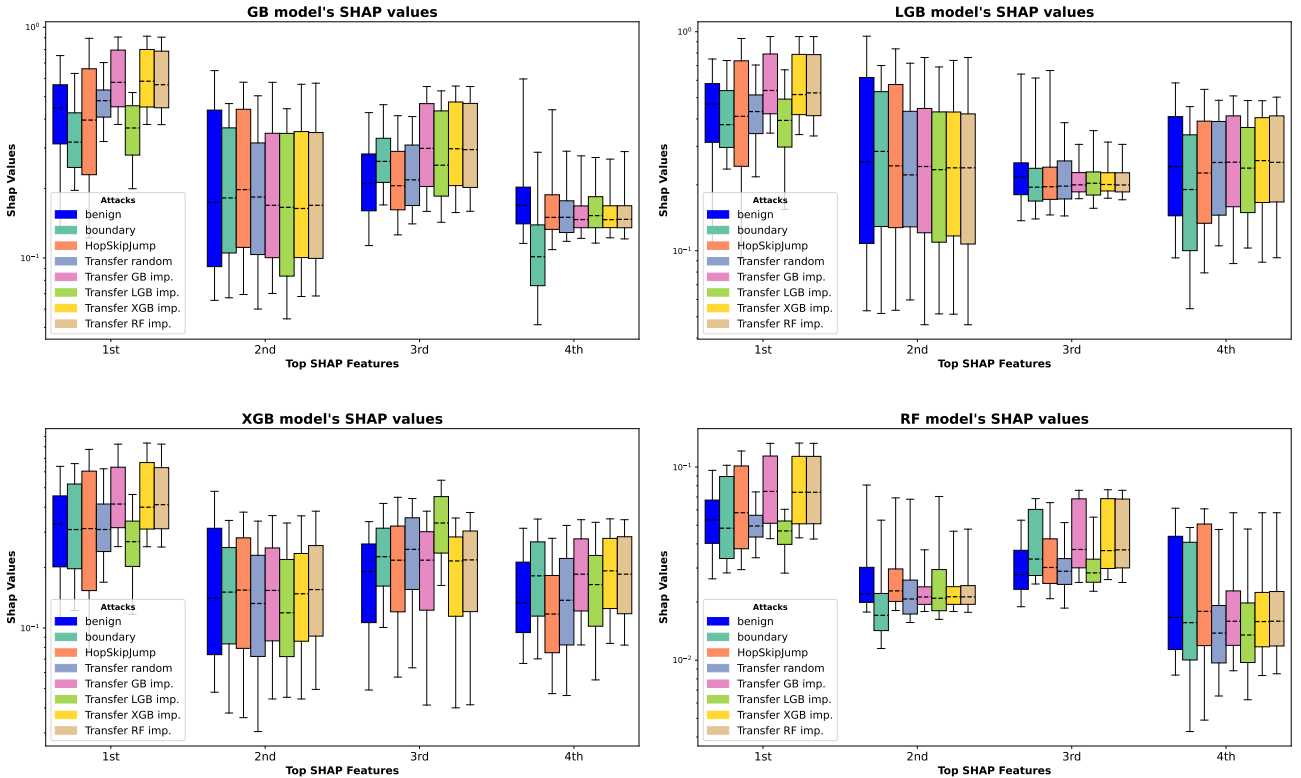


Figure 5: Attacks' quality evaluated based on the impact on the target model's decision-making process; SHAP value distribution for benign (blue) and adversarial samples (on the ICU dataset), across the top-four most important features selected based on their average SHAP values computed on the benign training dataset.

overhead but less effective in terms of success rate, especially on more challenging datasets like VideoTQ. The lower attack success rates for transferability-based attacks on the evaluated datasets highlight their limitations in adversarial scenarios.

In terms of attack quality, transferability-based attacks typically produce more coherent adversarial samples than the examined query-based attacks, as indicated by lower anomaly detection rates and subtler impacts on the target model's decision-making process, particularly on the Hate and ICU datasets. This is further supported by SHAP analysis, which reveals fewer anomalous features in these samples. These findings suggest that transferability-based attacks are inherently less detectable. The random-based selection attack is an exception, as it compromises coherence by arbitrarily modifying features, often resulting in anomalous values and noticeable shifts in SHAP values.

From a defender's perspective, however, transferability-based attacks present a unique challenge. Despite the lower transfer success rate, when adversarial samples generated by a surrogate model do manage to deceive the target model, they may be more challenging to detect, underscoring the complexity of defending against these types of attacks.

Interestingly, while low L_2 distances are commonly regarded in the literature as indicative of imperceptibility, our findings suggest this may not hold for tabular data. In

some cases, transferability-based attacks that achieved very low L_2 distances were still detected as anomalies by the AE. This finding calls into question the assumption that lower L_2 norms correlate with indistinguishability in tabular data domains, where imperceptibility may depend on other factors beyond the L_2 distance.

In this paper, we introduced two methods for evaluating the anomaly detection rate of black-box adversarial attacks: one based on an AE and the other on an IF model. Our results indicated that the AE model tended to identify a greater number of adversarial samples as anomalies than the IF model. This can be attributed to the nature of these models; the AE is a neural network capable of capturing more complex patterns, while the IF, a tree-based model, learns simpler patterns. These findings suggest that AE is more adept at learning benign data patterns, enabling it to identify a larger portion of adversarial samples as anomalous.

7. Conclusion

In this study we compare different attacks' strategies of black-box adversarial attacks on ML models for tabular data. Our evaluation framework considers the attacker's risk, effort, and the quality of adversarial samples, providing insights for both attack optimization and defense strategies.

Results across diverse target models and datasets reveal distinct trade-offs: query-based attacks, while highly

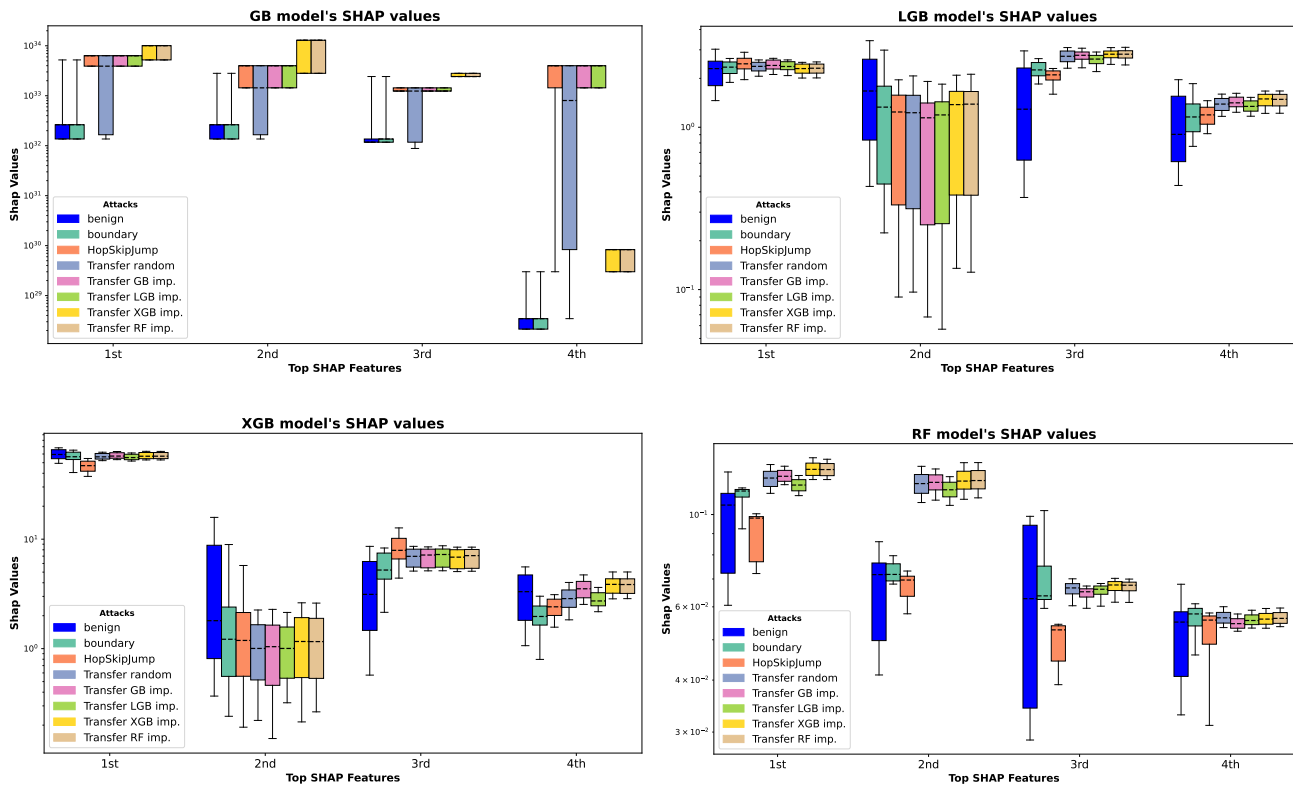


Figure 6: Attacks' quality evaluated based on the impact on the target model's decision-making process; SHAP value distribution for benign (blue) and adversarial samples (on the **VideoTQ** dataset), across the top-four most important features selected based on their average SHAP values computed on the benign training dataset.

effective, often sacrifice coherence by leading to significant distortions, and require substantial computational resources. Transferability-based attacks, though less successful in some cases, achieve greater coherence with fewer feature modifications and a subtler impact on model decision-making, as reflected in lower anomaly detection rates and minimal disruptions to feature importance.

Balancing coherence and effectiveness is thus essential in adversarial attack design, especially when deploying query-based attacks on models that use them as a defense strategy for tabular data. The metrics introduced in this paper to evaluate adversarial samples and attacks in the tabular domain provide a foundation for further research. This can help develop a more balanced approach that maximizes the attack effectiveness of transferability-based attacks while maintaining the input integrity of query-based attacks, ultimately aiding defenders in strengthening their defenses.

Future work may explore adversarial robustness in more complex ML pipelines in the tabular domain, such as those where models incorporate defenses against such attacks, or where the attacker does not have knowledge of all the target model's features.

8. Declarations

The authors declare that they have no known competing financial interests or personal relationships that could have appeared to influence the work reported in this paper.

Appendix A Pseudocode for Tabular Attacks

In this research, we applied two types of query-based attacks: the Boundary and HopSkipJump attacks, along with five versions of transferability-based attack, all adapted for the tabular domain and outlined below.

In the Boundary attack presented in Algorithm 1, the attacker randomly selects a sample from the defined target class, regardless of its proximity to the original sample (lines 2-3). The attacker then optimizes the modified sample's values using an orthogonal perturbation, which iteratively adjusts the feature values to minimize the model's confidence in the original class while ensuring that the predicted class is the target class (lines 4-6). During the crafting process, tabular constraints are applied to the sample (see Algorithm 2), projecting each feature value onto its closest legitimate value to ensure input validity (line 7).

In contrast, in the HopSkipJump attack, which is presented in Algorithm 3, the attacker employs binary search and proceeds in the target class gradients' direction to find a sample from the defined target class with the closest

Algorithm 1: The Boundary adversarial attack for tabular data

Input: The target model M , original sample x , original sample’s true label y , set of immutable features I , set of each feature constraints $Constraints$, and the similarity threshold α

```

1  $x^{adv} \leftarrow x$ 
2 while  $i < max\_init\_steps \wedge M(x^{adv}) = y$  do
3    $x^{adv} \leftarrow$  random perturbation from distribution
    $x \sim \mathcal{N}(\mu, \sigma^2)$ 
  end
4 while  $i < max\_iteration\_steps \wedge M(x^{adv}) = y \wedge$ 
    $Similarity(x, x^{adv}) < \alpha$  do
5   while  $j < max\_similarity\_steps$  do
6      $x^{adv} \leftarrow x^{adv} +$ 
     Orthogonal_Perturbation( $x, x^{adv}$ )
   end
7    $x^{adv} \leftarrow$  Tabular_Modify( $x, x^{adv}, I, Constraints,$ 
   regression_models)
  end
8 return  $x^{adv}$ 

```

Algorithm 2: A generic procedure for applying constraints of tabular data domains

Input: The original sample x , adversarial sample x^{adv} , set of immutable features I , and the set of each feature constraints $Constraints$

```

1 Procedure Tabular_Modify( $x, x^{adv}, I, Constraints,$ 
  regression_models)
2   Clip (min, max)
3   Impose realistic values (constraints)
4   Impose immutable features (I)
5   Correct dependent features (regression_models)
6   return adversarial

```

proximity to the original sample (lines 5-10). During the binary search, tabular constraints are applied to the sample (see Algorithm 2), projecting each feature value onto its closest legitimate value to ensure input validity (line 11).

In our evaluation, we implemented untargeted transferability-based gradient attacks based on the architecture in [35, 19], and the pseudocode is presented in Algorithm 4. The attacker first selects the feature likely to have the most impact on the model’s prediction, excluding immutable features, i.e., features that cannot be changed by the attacker (line 4). The selection, which is presented in lines 9-13, can be made by: 1) selecting k random features and the n features that are most correlated with them [35]. 2-4) using a feature importance technique to select the k most important features [19] and the n features that are most correlated with them. The feature importance technique can be performed by training an ML classifier (such as GB, XGB, LGB, and RF models) and extracting what they

Algorithm 3: The HopSkipJump adversarial attack for tabular data

Input: The target model M , original sample x , original sample’s true label y , set of immutable features I , set of each feature constraints $Constraints$, and the similarity threshold α

```

1  $x^{adv} \leftarrow x$ 
2 while  $i < max\_init\_steps \wedge M(x^{adv}) = y$  do
3    $x^{adv} \leftarrow$  random perturbation from distribution
    $x \sim \mathcal{N}(\mu, \sigma^2)$ 
4    $x^{adv} \leftarrow$  Binary_Search( $x, x^{adv}$ )
  end
5 while  $i < max\_iteration\_steps \wedge M(x^{adv}) = y \wedge$ 
    $Similarity(x, x^{adv}) < \alpha$  do
6   while  $j < max\_similarity\_steps$  do
7      $x^{adv} \leftarrow$  Binary_Search( $x, x^{adv}$ )
8     update  $\leftarrow$  Compute_Update( $x, x^{adv}$ )
9     potential_sample  $\leftarrow$  run step size search
     ( $x^{adv}, update$ ) until predicts satisfying
10     $x^{adv} \leftarrow$  potential_sample
  end
11   $x^{adv} \leftarrow$  Tabular_Modify( $x, x^{adv}, I, Constraints$ )
  end
12 return  $x^{adv}$ 

```

consider the most important features [19]. After selecting features to perturb, a perturbation vector p is calculated for the selected features by using an optimizer that minimizes the adversary’s objective function (line 5). Finally, tabular constraints are applied to the sample (see Algorithm 2), projecting each feature value onto its closest legitimate value to ensure input validity (line 7).

CRediT authorship contribution statement

Yael Itzhakev: Writing – review & editing, Writing – original draft, Visualization, Data curation, Investigation, Formal analysis, Validation, Software, Methodology, Conceptualization. **Amit Giloni:** Writing – review & editing, Validation, Conceptualization. **Yuval Elovici:** Supervision. **Asaf Shabtai:** Supervision, Project administration.

Algorithm 4: An untargeted transferability-based adversarial attack for tabular data

Input: The target model M , original sample x , original sample's true label y , adversary's objective loss function L^{adv} , set of immutable features I , set of each feature constraints $Constraints$, maximum allowed L_0 -perturbation noise λ , number of most important features to perturb k , and number of features most correlated with the k features chosen n

```
1  $x^{adv} \leftarrow x$ 
2  $F \leftarrow \emptyset$ 
3 while  $M'(x^{adv}) = y \wedge |F| < \lambda$  do
4    $F \leftarrow FU\ Select\_Features(M', x^{adv}, I, F, k, n)$ 
5    $p \leftarrow Compute\_Perturbation(M', L^{adv}, x^{adv}, F)$ 
6    $x_i^{adv} \leftarrow x_i^{adv} + p$ 
7    $x^{adv} \leftarrow$ 
    $Tabular\_Modify(x, x^{adv}, I, Constraints)$ 
8 return  $x^{adv}$ 

Procedure  $Select\_Features(M', x^{adv}, I, F, k, n)$ 
9   •Random-Based Selection
10  •GB Feature Importance-Based Selection
11  •XGB Feature Importance-Based Selection
12  •LGB Feature Importance-Based Selection
13  •RF Feature Importance-Based Selection
```

References

- [1] Alecci, M., Conti, M., Marchiori, F., Martinelli, L., Pajola, L., 2023. Your attack is too dumb: Formalizing attacker scenarios for adversarial transferability, in: Proceedings of the 26th International Symposium on Research in Attacks, Intrusions and Defenses, pp. 315–329.
- [2] Ballet, V., Renard, X., Aigrain, J., Laugel, T., Frossard, P., Detyniecki, M., 2019. Imperceptible adversarial attacks on tabular data. arXiv preprint arXiv:1911.03274 .
- [3] Belle, V., Papantonis, I., 2021. Principles and practice of explainable machine learning. *Frontiers in big Data* , 39.
- [4] Breiman, L., 2001. Random forests. *Machine learning* 45, 5–32.
- [5] Brendel, W., Rauber, J., Bethge, M., 2017. Decision-based adversarial attacks: Reliable attacks against black-box machine learning models. arXiv preprint arXiv:1712.04248 .
- [6] Byun, J., Go, H., Kim, C., 2022. On the effectiveness of small input noise for defending against query-based black-box attacks, in: Proceedings of the IEEE/CVF Winter Conference on Applications of Computer Vision, pp. 3051–3060.
- [7] Cartella, F., Anunciacao, O., Funabiki, Y., Yamaguchi, D., Akishita, T., Elshocht, O., 2021. Adversarial attacks for tabular data: Application to fraud detection and imbalanced data. arXiv preprint arXiv:2101.08030 .
- [8] Chen, J., Jordan, M.L., Wainwright, M.J., 2020. Hopskipjumpattack: A query-efficient decision-based attack, in: 2020 IEEE Symposium on Security and Privacy (SP), IEEE. pp. 1277–1294.
- [9] Chen, T., Guestrin, C., 2016. Xgboost: A scalable tree boosting system, in: Proceedings of the 22nd ACM SIGKDD International Conference on Knowledge Discovery and Data Mining, pp. 785–794.
- [10] Chen, X., Liu, C., Zhao, Y., Jia, Z., Jin, G., 2022. Improving adversarial robustness of bayesian neural networks via multi-task adversarial training. *Information Sciences* 592, 156–173.
- [11] Crouhy, M., Galai, D., Mark, R., 2000. A comparative analysis of current credit risk models. *Journal of Banking & Finance* 24, 59–117.
- [12] Danese, M.D., Halperin, M., Duryea, J., Duryea, R., 2019. The generalized data model for clinical research. *BMC medical informatics and decision making* 19, 1–13.
- [13] Deldjoo, Y., Noia, T.D., Merra, F.A., 2021. A survey on adversarial recommender systems: from attack/defense strategies to generative adversarial networks. *ACM Computing Surveys (CSUR)* 54, 1–38.
- [14] Fezza, S.A., Bakhti, Y., Hamidouche, W., Déforges, O., 2019. Perceptual evaluation of adversarial attacks for cnn-based image classification, in: 2019 Eleventh International Conference on Quality of Multimedia Experience (QoMEX), IEEE. pp. 1–6.
- [15] Friedman, J.H., 2001. Greedy function approximation: a gradient boosting machine. *Annals of statistics* , 1189–1232.
- [16] Gómez, A.L.P., Maimó, L.F., Celdrán, A.H., Clemente, F.J.G., 2023. Vaasi: Crafting valid and abnormal adversarial samples for anomaly detection systems in industrial scenarios. *Journal of Information Security and Applications* 79, 103647.
- [17] Goodfellow, I.J., Shlens, J., Szegedy, C., 2014. Explaining and harnessing adversarial examples. arXiv preprint arXiv:1412.6572 .
- [18] Goyal, S., Doddapaneni, S., Khapra, M.M., Ravindran, B., 2023. A survey of adversarial defenses and robustness in nlp. *ACM Computing Surveys* 55, 1–39.
- [19] Grolman, E., Binyamini, H., Shabtai, A., Elovici, Y., Morikawa, I., Shimizu, T., 2022. Hateversarial: Adversarial attack against hate speech detection algorithms on twitter, in: Proceedings of the 30th ACM Conference on User Modeling, Adaptation and Personalization, pp. 143–152.
- [20] Hanberger, H., Monnet, D.L., Nilsson, L.E., 2005. Intensive care unit, in: *Antibiotic policies: theory and practice*. Springer, pp. 261–279.
- [21] Haroon, M.S., Ali, H.M., 2022. Adversarial training against adversarial attacks for machine learning-based intrusion detection systems. *Computers, Materials & Continua* 73.
- [22] Ilyas, A., Engstrom, L., Athalye, A., Lin, J., 2018. Black-box adversarial attacks with limited queries and information, in: *International conference on machine learning*, PMLR. pp. 2137–2146.
- [23] Ju, L., Cui, R., Sun, J., Li, Z., 2022. A robust approach to adversarial attack on tabular data for classification algorithm testing, in: 2022 8th International Conference on Big Data and Information Analytics (BigDIA), IEEE. pp. 371–376.
- [24] Kaviani, S., Han, K.J., Sohn, I., 2022. Adversarial attacks and defenses on ai in medical imaging informatics: A survey. *Expert Systems with Applications* 198, 116815.
- [25] Ke, G., Meng, Q., Finley, T., Wang, T., Chen, W., Ma, W., Ye, Q., Liu, T.Y., 2017. Lightgbm: A highly efficient gradient boosting decision tree. *Advances in neural information processing systems* 30.
- [26] Kingma, D.P., Ba, J., 2014. Adam: A method for stochastic optimization. arXiv preprint arXiv:1412.6980 .
- [27] Kurakin, A., Goodfellow, I.J., Bengio, S., 2018. Adversarial examples in the physical world, in: *Artificial intelligence safety and security*. Chapman and Hall/CRC, pp. 99–112.
- [28] Lam, J.C., Wan, K.K., Cheung, K., Yang, L., 2008. Principal component analysis of electricity use in office buildings. *Energy and buildings* 40, 828–836.
- [29] Lan, J., Zhang, R., Yan, Z., Wang, J., Chen, Y., Hou, R., 2022. Adversarial attacks and defenses in speaker recognition systems: A survey. *Journal of Systems Architecture* 127, 102526.
- [30] Liu, F.T., Ting, K.M., Zhou, Z.H., 2008. Isolation forest, in: 2008 eighth IEEE international conference on data mining, IEEE. pp. 413–422.
- [31] Liu, L., Qi, H., 2017. Learning effective binary descriptors via cross entropy, in: 2017 IEEE winter conference on applications of computer vision (WACV), IEEE. pp. 1251–1258.
- [32] Lundberg, S.M., Lee, S.I., 2017. A unified approach to interpreting model predictions. *Advances in neural information processing systems* 30.
- [33] Mahmood, K., Mahmood, R., Rathbun, E., van Dijk, M., 2021. Back in black: A comparative evaluation of recent state-of-the-art black-box

- attacks. *IEEE Access* 10, 998–1019.
- [34] Marulli, F., Verde, L., Campanile, L., 2021. Exploring data and model poisoning attacks to deep learning-based nlp systems. *Procedia Computer Science* 192, 3570–3579.
- [35] Mathov, Y., Levy, E., Katzir, Z., Shabtai, A., Elovici, Y., 2022. Not all datasets are born equal: On heterogeneous tabular data and adversarial examples. *Knowledge-Based Systems* 242, 108377.
- [36] Moro, S., Laureano, R., Cortez, P., 2011. Using data mining for bank direct marketing: An application of the crisp-dm methodology .
- [37] Nicolae, M.I., Sinn, M., Tran, M.N., Buesser, B., Rawat, A., Wistuba, M., Zantedeschi, V., Baracaldo, N., Chen, B., Ludwig, H., et al., 2018. Adversarial robustness toolbox v1. 0.0. *arXiv preprint arXiv:1807.01069* .
- [38] Papernot, N., McDaniel, P., Goodfellow, I., Jha, S., Celik, Z.B., Swami, A., 2017. Practical black-box attacks against machine learning, in: *Proceedings of the 2017 ACM on Asia conference on computer and communications security*, pp. 506–519.
- [39] Papernot, N., McDaniel, P., Jha, S., Fredrikson, M., Celik, Z.B., Swami, A., 2016. The limitations of deep learning in adversarial settings, in: *2016 IEEE European symposium on security and privacy (EuroS&P)*, IEEE. pp. 372–387.
- [40] Pennington, J., Socher, R., Manning, C.D., 2014. Glove: Global vectors for word representation, in: *Proceedings of the 2014 conference on empirical methods in natural language processing (EMNLP)*, pp. 1532–1543.
- [41] Puttagunta, M.K., Ravi, S., Nelson Kennedy Babu, C., 2023. Adversarial examples: attacks and defences on medical deep learning systems. *Multimedia Tools and Applications* , 1–37.
- [42] Ramesh, T., Prakash, R., Shukla, K., 2010. Life cycle energy analysis of buildings: An overview. *Energy and buildings* 42, 1592–1600.
- [43] Ribeiro, M., Calais, P., Santos, Y., Almeida, V., Meira Jr, W., 2018. Characterizing and detecting hateful users on twitter, in: *Proceedings of the International AAAI Conference on Web and Social Media*.
- [44] Sakurada, M., Yairi, T., 2014. Anomaly detection using autoencoders with nonlinear dimensionality reduction, in: *Proceedings of the MLSDA 2014 2nd workshop on machine learning for sensory data analysis*, pp. 4–11.
- [45] Sun, L., Dou, Y., Yang, C., Zhang, K., Wang, J., Philip, S.Y., He, L., Li, B., 2022. Adversarial attack and defense on graph data: A survey. *IEEE Transactions on Knowledge and Data Engineering* .
- [46] Szegedy, C., Zaremba, W., Sutskever, I., Bruna, J., Erhan, D., Goodfellow, I., Fergus, R., 2013. Intriguing properties of neural networks. *arXiv preprint arXiv:1312.6199* .
- [47] Wang, Q., Zheng, B., Li, Q., Shen, C., Ba, Z., 2020. Towards query-efficient adversarial attacks against automatic speech recognition systems. *IEEE Transactions on Information Forensics and Security* 16, 896–908.
- [48] Weisstein, E.W., 2006. Correlation coefficient. <https://mathworld.wolfram.com/> .
- [49] Xu, H., Ma, Y., Liu, H.C., Deb, D., Liu, H., Tang, J.L., Jain, A.K., 2020. Adversarial attacks and defenses in images, graphs and text: A review. *International Journal of Automation and Computing* 17, 151–178.
- [50] Zizzo, G., Hankin, C., Maffei, S., Jones, K., 2019. Adversarial machine learning beyond the image domain, in: *Proceedings of the 56th Annual Design Automation Conference 2019*, pp. 1–4.